Na+/Ca2+ exchanger isoform 1 takes part to the Ca2+-related prosurvival pathway of SOD1 in primary motor neurons exposed to beta-methylamino-L-alanine

Agnese Secondo (secondo@unina.it)
University of Naples Federico II: School of Medicine https://orcid.org/0000-0001-5054-4098
Tiziana Petrozziello
University of Naples Federico II Faculty of Engineering: Universita degli Studi di Napoli Federico II
Francesca Boscia
University of Naples Federico II: Universita degli Studi di Napoli Federico II
Valentina Tedeschi
University of Naples Federico II: Universita degli Studi di Napoli Federico II
Anna Pannaccione
University of Naples Federico II: Universita degli Studi di Napoli Federico II
Valeria de Rosa
University of Naples Federico II: Universita degli Studi di Napoli Federico II
Angela Corvino
University of Naples Federico II Department of Pharmacy: Universita degli Studi di Napoli Federico II Dipartimento di Farmacia
Beatrice Severino
University of Naples Federico II Department of Pharmacy: Universita degli Studi di Napoli Federico II Dipartimento di Farmacia
Lucio Annunziato
SDN Foundation: Fondazione SDN

Research

Keywords: L-BMAA, NCX1, SOD1, calcium signaling, neuroprotection ApoSOD1

Posted Date: July 28th, 2021

DOI: https://doi.org/10.21203/rs.3.rs-715721/v1

Na^+/Ca^{2+} exchanger isoform 1 takes part to the Ca^{2+}-related prosurvival pathway of SOD1 in primary motor neurons exposed to beta-methylamino-L-alanine

Tiziana Petrozziello[1], Francesca Boscia[1], Valentina Tedeschi[1], Anna Pannaccione[1], Valeria de Rosa[1], Angela Corvino[2], Beatrice Severino[2], Lucio Annunziato[3], Agnese Secondo[1*]

* Correspondence: secondo@unina.it; Tel.: +39-081-7463335

Affiliations:
[1]Division of Pharmacology, Department of Neuroscience, Reproductive and Odontostomatological Sciences, School of Medicine, "Federico II" University of Naples, Via S. Pansini 5, 80131, Naples, Italy
[2]Department of Pharmacy, School of Medicine, University of Naples Federico II, Naples, Italy
[3]IRCCS SDN, 80143 Naples, Italy

One Sentence Summary: NCX1 activation neuroprotects against L-BMAA

tiziana.petrozziello@unina.it

boscia@unina.it

valentina.tedeschi@unina.it

pannacio@unina.it

derosa@unina.it

angela.corvino@unina.it

severino@unina.it

annunzi@unina.it

secondo@unina.it

Abstract

Background: The cycad neurotoxin beta-methylamino-L-alanine (L-BMAA), causing the amyotrophic lateral sclerosis/Parkinson-dementia complex (ALS/PDC), may cause neurodegeneration by disrupting organellar Ca^{2+} homeostasis. By activating Akt/ERK1/2 pathway, the Cu,Zn-superoxide dismutase (SOD1) and its non-metallated form, ApoSOD1, prevent endoplasmic reticulum (ER) stress-induced cell death in motor neurons exposed to L-BMAA. This occurs through the rapid increase of intracellular Ca^{2+} concentration ($[Ca^{2+}]_i$) in part flowing from the extracellular compartment and in part released from ER. However, the molecular components of this mechanism remain uncharacterized.

Methods: By an integrated approach consisting on the use of siRNA strategy, Western blotting, confocal double labeling immunofluorescence, patch-clamp electrophysiology, and Fura 2-/SBFI-single-cell imaging, we explored in rat motor neuron-enriched cultures the involvement of plasma membrane Na^+/Ca^{2+} exchanger (NCX) and the purinergic P_2X_7 receptor as well as of the intracellular cADP-ribose (cADPR) pathway in the rapid and neuroprotective mechanism of SOD1.

Results: we showed that SOD1-induced $[Ca^{2+}]_i$ rise was prevented by the pan inhibitor of NCX CB-DMB but not by A430879, a P_2X_7 receptor specific antagonist, or by 8-bromo-cADPR, a cell permeant antagonist of cADP-ribose. The same occurred for the ApoSOD1. Confocal double labeling immunofluorescence showed a huge expression of plasmalemmal NCX1 and intracellular NCX3 isoforms. Furthermore, we identified NCX1 reverse mode as the main mechanism responsible for the neuroprotective ER Ca^{2+} refilling elicited by SOD1 and ApoSOD1. Furthermore, SOD1 and ApoSOD1 promoted translocation of active Akt in some nuclei of primary motor neurons. Finally, the activation of NCX1 by the specific agonist CN-PYB2 protected motor neurons from L-BMAA-induced cell death.

Conclusion: collectively, our data indicate that SOD1 and ApoSOD1 exert their neuroprotective effect by modulating ER Ca^{2+} content through the activation of NCX1 reverse mode and Akt nuclear translocation in a subset of primary motor neurons.

Background

Calcium (Ca^{2+}) imbalance is now considered one of the key elements of the neurodegenerative process occurring in amyotrophic lateral sclerosis (ALS), a fatal adult-onset disease characterized by progressive degeneration of both upper and lower motor neurons (*1, 2*). Accordingly, during the disease progression, dysfunctional Ca^{2+} homeostasis may lead to misfolding of several proteins (*3*), thus facilitating their toxic aggregation. Importantly, organellar Ca^{2+} homeostasis, with particular respect to the endoplasmic reticulum (ER), is compromised in ALS preclinical models and is now considered a relevant pathogenic mechanism of the disease (*4, 5*). About 20% of cases of familial form (fALS) and 2-7% of sporadic form of ALS (sALS) are caused by mutations in the gene encoding the cytosolic Cu,Zn-superoxide dismutase (SOD1). This makes *sod1* the second most frequently mutated gene after *C9orf72* in ALS Caucasian patients (*6-8*) (http://alsod.iop.kcl.ac.uk/). While mutated SOD1 accumulates as unfolded trimers causing motor neuron degeneration (*9*), dysfunctional secretion of native wild-type SOD1 may also favor the neurodegeneration in ALS (*10*). In fact, a chronic intraspinal infusion of wild-type SOD1 significantly delays disease progression in transgenic animals carrying mutant human $SOD1^{G93A}$ (*10*). Furthermore, mutant SOD1 may induce ER stress by targeting several molecular components of ER-associated degradation (ERAD) machinery (*11*). On the other hand, a rapid exposure to wild type SOD1 may protect motor neurons against ER stress induced by the beta-methylamino-L-alanine (L-BMAA) (*12*), a neurotoxin causing the Guamanian form of ALS (*13*). Interestingly, the activation of Akt/ERK1/2 pathway *via* a transient [Ca^{2+}] rise may underline the protective effect of SOD1 (*12*). Mechanicistically, this neuroprotective effect is independent from the catalytic activity of the enzyme, since the non-metallated form ApoSOD1, lacking dismutase activity, may induce protection of motor neurons from L-BMAA toxicity likewise SOD1 (*12*). Therefore, considering that the neuroprotection exerted by SOD1 and ApoSOD1 may pass through a rapid and transient $[Ca^{2+}]_i$ increase, in the present study we investigated, by a pharmacological and siRNA approach, the involvement of the Na^+/Ca^{2+} exchanger isoforms (NCXs), the cyclic adenosine diphosphate-ribose (cADPR) receptor and the purinergic receptor P_2X_7, most of which are implicated in the pathogenesis of ALS.

Keywords: L-BMAA, NCX1, SOD1, calcium signaling, neuroprotection ApoSOD1

Methods

Reagents. Media, sera, and antibiotics for cell cultures were purchased from Life Technologies (Milan, Italy). Mouse monoclonal anti-p-Akt (#4051) was from Cell Signaling Technology Inc. (Danvers, MA, USA). Rabbit polyclonal antibody against Akt1/2/3 (#sc-8312) was from Santa Cruz Biotechnology, Inc. (Dallas, TX, USA). Rabbit polyclonal antibody against NCX1 (#π11-13) was from Swant (Bellinzona, Switzerland); rabbit polyclonal anti-NCX3 antibody was done by Dr. K. Philipson (University of California, Los Angeles, CA, USA). Mouse monoclonal anti-SOD (#S2147) and rabbit polyclonal anti-MAP2 (#M3696) antibodies were from Sigma-Aldrich (Milan, Italy). ECL reagents and nitrocellulose membranes were from GE Healthcare (Milan, Italy). SOD1, retinoic acid, L-BMAA, thapsigargin, H2O2, 8-bromo-cADPR, and all other reagents were from Sigma-Aldrich (Milan, Italy). A430879 was a kind gift from Prof. Santina Bruzzone (Department of Experimental Medicine, University of Genova, Genova, Italy). Fura-2/AM and SBFI/AM were from Life Technologies (Milan, Italy).

Rat primary motor neurons. Motor neuron-enriched cultures were obtained from the spinal cord of 12-14-day-old Wistar rat embryos and cultured as previously described (12, 43). Cytosine β-D-arabinofuranoside hydrochloride (Ara-C, 10 μM) was added at 4 and 8 DIV (days in vitro) to prevent non-neuronal cell growth. Primary motor neurons were kept at 37°C in a humidified 5% CO2 atmosphere and used after 10-12 DIV. All the procedures were performed according to the experimental protocols approved by the Ethical Committee of "Federico II" University of Naples, Italy, and according to the guidelines and regulations by Italian Ministry of Health (D.Lgs. March 4th, 2014 from Italian Ministry of Health and DIR 2010/63 from UE).

Hybrid cell line. NSC-34 motor neurons were grown in Dulbecco's Modified Eagles Medium (DMEM) containing 10% fetal bovine serum (FBS), 2 mM L-glutamine, 100 IU/ml penicillin, and 100 μg/ml streptomycin, and kept in a 5% CO2 and 95% air atmosphere at 37°C. Before each experiment, NSC-34 cells were differentiated in 10 μM retinoic acid for 48 h, thus triggering a typical neuronal phenotype (44).

SOD1 inactivation. SOD1 was incubated with 200 mM H2O2 in 25 mM sodium bicarbonate buffer (pH 7.5) for 2 h at room temperature (RT). At the end, the reaction was stopped by adding 1000 U/ml catalase for 30 min at 37°C. Finally, SOD1 activity was measured by the SOD assay kit purchased from Sigma-Aldrich (Milan, Italy), as previously described (12).

[Ca2+]i and [Na+]i measurements. [Ca2+]i was measured by single cell computer-assisted video-imaging in NSC-34 motor neurons and in primary motor neurons, as previously reported (35). Results are presented as cytosolic Ca2+ concentration calculated by the equation of Grynkiewicz et al. (45, 46). NCX activity was evaluated as Ca2+ uptake through the reverse mode by using a Na+-deficient N-methyl-D-glucamine (NMDG) solution (Na+-free) containing (in mM): 5.5 KCl, 147 NMDG, 1.2 MgCl2, 1.5 CaCl2, 10 glucose, and 10 HEPES (pH 7.4). The irreversible and selective inhibitor of the sarco(endo)plasmic reticulum Ca2+-ATPase (SERCA) thapsigargin (Tg; 1 μM) was added 10 min before the beginning of the recordings, as previously described (35). NCX activity was calculated as Δ% of peak/basal [Ca2+]i values after perfusion with a Na+-free solution. [Na+]i measurement was performed by loading motor neurons with 10 μM SBFI/AM incubated in the presence of 0.02% pluronic acid for 1 h at 37°C (36).

Patch-clamp electrophysiology. NCX currents (INCX) in motor neurons were recorded by patch-clamp technique in whole-cell configuration using the commercially available amplifier Axopatch200B and Digidata1322A interface (Molecular Devices), as previously described (35,

47, 48). INCX was recorded starting from a holding potential of −60 mV up to a short-step depolarization at +60 mV (60 ms). A descending voltage ramp from +60 mV to −120 mV was applied. INCX recorded in the descending portion of the ramp (from +60 mV to −120 mV) was used to plot the current–voltage (I–V) relation curve. The INCX magnitude was measured at the end of +60 mV (reverse mode) and at the end of −120 mV (forward mode), respectively. To isolate INCX, the same cells were recorded first for total currents and then for currents in the presence of Ni2+ (5 mM), a selective blocker of INCX. To obtain the isolated INCX, the Ni2+-insensitive unspecific currents were subtracted from the total currents (INCX = IT − INiResistant) (35, 47, 48). Motor neurons were perfused with external Ringer's solution containing the following (in mM): 126 NaCl, 1.2 NaHPO4, 2.4 KCl, 2.4 CaCl2, 1.2 MgCl2, 10 glucose, and 18 NaHCO3 (pH 7.4). Twenty millimolar tetraethylammonium (TEA), 50 nM tetradotoxin (TTX), and 10 μM nimodipine were added to Ringer's solution to abolish potassium, sodium, and calcium currents. The dialyzing pipette solution contained the following (in mM): 100 K-gluconate, 10 TEA, 20 NaCl, 1 Mg-ATP, 0.1 CaCl2, 2 MgCl2, 0.75 EGTA, and 10 HEPES (pH 7.2). Membrane capacitance was calculated according to the following equation: $Cm = \tau c \bullet Io/\Delta Em(1 - I\infty/Io)$, where Cm is membrane capacitance, τc is the time constant of the membrane capacitance, Io is the maximum capacitance current value, ΔEm is the amplitude of the voltage step, and I∞ is the amplitude of the steady state current (36).

Immunocytochemistry. Motor neurons were cultured on glass coverslips for 12 days. Then, cells were rinsed twice in cold 0.01 M PBS (pH 7.4) and fixed in 4% (w/v) paraformaldehyde (Sigma-Aldrich, Milan, Italy) for 20 min at RT. After three washes in PBS, cells were blocked with 3% (w/v) BSA and 0.05% Triton-X (Bio-Rad, Milan, Italy) for 1 h at RT. Coverslips were then incubated overnight at 4°C with the following primary antibodies: rabbit polyclonal antibody against NCX1 (#π11-13, Swant, Bellinzona, Switzerland), rabbit polyclonal antibody against NCX3 (Dr. K. Philipson Laboratory, University of California, Los Angeles, CA, USA), mouse monoclonal antibody against SOD (#S2147, Sigma-Aldrich, Milan, Italy), mouse monoclonal antibody against p-Akt (#4051, Cell Signaling Technology Inc., Danvers, MA, USA), or rabbit polyclonal antibody against MAP2 (#M3696, Sigma-Aldrich, Milan, Italy). After three washes in PBS, coverslips were incubated in the dark with the corresponding secondary antibodies for 1 h at RT. After the final wash, coverslips were mounted with Vectashield (Vector Labs, Burlingame, CA) and analyzed with a Nikon Eclipse 400 upright microscope (Nikon Instruments, Florence, Italy), equipped with a CCD digital camera (Coolsnap-Pro, Media Cybernetics, Silver Springs, MD, USA) and Image Pro-Plus software (Media Cybernetics, Silver Springs, MD, USA).

Small interfering RNA. NCX1 and NCX3 knocking down was obtained by siRNA duplex against NCX1 or NCX3 and their non-targeting control (Qiagen, Milan, Italy), as previously described (49, 50). Motor neurons were transfected for 5 h with each duplex at a final concentration of 10 nM using HiPerFect transfection reagent (Qiagen, Milan, Italy).

L-BMAA treatment and cell viability measurement. Primary cultures of motor neurons were exposed to 300 μM L-BMAA for 48 h. SOD1 (400 ng/ml) or ApoSOD1 (400 ng/ml) were added in fresh medium 10 minutes before L-BMAA addition, while the specific NCX1 activator, CN-PYB2 (10 nM) (26), was added in fresh medium together with the neurotoxin. After 48 h exposure to L-BMAA, mitochondrial activity was evaluated by the MTT (3[4,5-dimethylthiazol-2-yl]-2,5-diphenyl-tetrazolium bromide) assay. Data are expressed as a percentage of cell viability of control cultures.

Western blotting. After treatments, cells were lysed in ice-cold lysis buffer containing 20 mM Tris-HCl (pH 7.5), 10 mM NaF, 1 mM phenylmethylsulfonyl fluoride, 1% NONIDET P-40, 1 mM Na3VO4, 0.1% aprotinin, 0.7 mg/ml pepstatin and 1 µg/ml leupeptin. Protein concentration of each sample was determined by the Bradford method (51). Proteins (50 µg) were separated on 10% SDS-polyacrylamide gels and transferred onto Hybond ECL nitrocellulose membranes (GE Healthcare, Milan, Italy). Membranes were blocked with 5% non-fat dry milk in 0.1% Tween 20 (Sigma-Aldrich, Milan, Italy) (2 mM Tris-HCl and 50 mM NaCl, pH 7.5) for 2 h at RT and then incubated overnight at 4°C in the blocking buffer containing the mouse monoclonal antibody against p-Akt (1:1000). Membranes were then re-blotted with the rabbit polyclonal antibody against Akt1/2/3 (1:1000). Immunoreactive bands were detected with the ECL reagent (GE Healthcare, Milan, Italy) and then the optical density of the bands was determined by Chemi-Doc Imaging System (Bio-Rad, Milan, Italy).

Statistical analysis. Data are expressed as mean ± S.E.M. Statistical comparisons between controls and treated experimental groups were performed using the one-way ANOVA, followed by Newman-Keuls test. $P<0.05$ was considered statistically significant.

Results

Plasma membrane Na^+/Ca^{2+} exchanger isoform 1 (NCX1) mediates rapid $[Ca^{2+}]_i$ increase induced by SOD1 and ApoSOD1 in rat primary motor neurons

SOD1 and its metal-free protein ApoSOD1 may induce the activation of Akt/ERK1/2 prosurvival pathway through a rapid increase of $[Ca^{2+}]_i$ in motor neuron-enriched cultures exposed to the neurotoxin L-BMAA (*12*). This effect is only partially reduced in a Ca^{2+}-free solution, suggesting the involvement of both intracellular and extracellular compartments (*12*). Therefore, we have investigated the putative involvement of three different targets regulating Ca^{2+} handling from extracellular to intracellular compartments: (a) purinergic P_2X_7 receptor (*14*), (b) cADP-ribose receptor (*15, 16*); and (c) Na^+/Ca^{2+} exchanger (NCX) (*17, 18*). Of interest, two of these proteins (i.e. P_2X_7 receptor and NCX) are mainly involved in ALS pathogenesis (*19-22*).

To verify the involvement of each of these ionic proteins in SOD1-dependent Ca^{2+}-signaling, rat primary motor neurons were exposed to SOD1 or ApoSOD1 in the presence of the specific antagonist of P_2X_7 receptor, A430879 (1μM) (*23*), the cell permeant antagonist of cADP-ribose named 8-bromo-cADPR (10μM) (*24*), or CB-DMB (1 μM), a pan inhibitor of NCX isoforms (*25*). These pharmacological tools were used at the respective IC_{50} for the proposed targets. Our results indicated that only CB-DMB significantly reduced the early increase of $[Ca^{2+}]_i$ induced by SOD1 (**Fig. 1A** and **B**) and ApoSOD1 (**Fig. 1C** and **D**). In contrast, A430879, blocking P_2X_7, and 8-bromo-cADPR, inhibiting cADP-ribose action, did not modify SOD1- (**Fig. 1B**) and ApoSOD1-induced $[Ca^{2+}]_i$ rise (**Fig. 1D**). This may suggest the involvement of NCX in the upstream mechanism of SOD1 and ApoSOD1 and possibly highlights the participation of the exchanger in their prosurvival effects against L-BMAA toxicity.

The activation of NCX1 reverse mode induced by SOD1 and ApoSOD1 is due to the $[Na^+]_i$ accumulation in rat primary motor neurons

In order to identify which isoform of NCX could be involved in the Ca^{2+}-dependent neuroprotective mechanism elicited by SOD1 and ApoSOD1, we analyzed the expression and activity of NCX1 and NCX3 isoforms in motor neuron-enriched cultures. As shown by confocal analysis in **Fig. 2A**, these isoforms were both significantly expressed in motor neurons. Also NSC-34 cells expressed high level of the exchanger isoform proteins (data not shown). However, in primary motor neurons, NCX1 was detected only on plasma membrane of the soma and neuronal processes, while NCX3 was mostly present in the whole intracellular compartment. In particular, the intracellular localization of NCX3 was prevalent in some motor neurons resembling motor neurons 2. Therefore, a clear co-localization between the two isoforms was only marginally observed (see **Fig. 2A**). Then, NCX activity was studied by exposing Fura-2/AM-loaded motor neurons to a Na^+-free solution forcing the exchanger to operate in the reverse mode mediating $[Ca^{2+}]_i$ increase (**Fig. 2B** and **C**). However, NCX1 knocking down produced by siNCX1 completely abolished Na^+-free-induced $[Ca^{2+}]_i$ rise, while NCX3 knocking down did not (**Fig. 2B** and **C**). Interestingly, in siNCX1-treated neurons a significant increase of basal $[Ca^{2+}]_i$ was detected if compared to siControl-treated neurons (**Fig. 2D**). Moreover, SOD1 immunosignal was detected in NCX1-positive motor neurons (**Fig. 2E**) in which a significant co-localization between NCX1 and endogenous SOD1 was observed at plasma membrane level (**Fig. 3A**). Moreover, in SBFI-loaded motor neurons, SOD1 (400 ng/mL) induced a significant

increase in $[Na^+]_i$ when compared to untreated controls (**Fig. 3B**). The same $[Na^+]_i$ rise was detected after a brief exposure to ApoSOD1 (400 ng/mL) (**Fig. 3B**).

Furthermore, NCX activity was potentiated by both SOD1 and ApoSOD1 added to a Na^+-free solution compared with control neurons exposed to Na^+-free alone (**Fig. 3C** and **D**). However, this Na^+-free-dependent activation of NCX was abolished in motor neurons previously silenced for NCX1 (**Fig. 3C** and **D**).

NCX1 reverse mode induced by SOD1 and ApoSOD1 determines ER Ca^{2+} entry in rat primary motor neurons

To study the mechanism of action of SOD1, NCX current was recorded by patch-clamp electrophysiology in whole cell configuration (**Fig. 4**). SOD1, as well as its metal-free protein ApoSOD1, determined a significant increase of NCX reverse mode measured at +60 mV (**Fig. 4A, B and C**). On the other hand, NCX forward mode, measured at -120 mV, was unaffected by SOD1 or ApoSOD1 perfusion (**Fig. 4A and B**). Moreover, the knocking down of NCX1 by siNCX1 not only reduced NCX total current in motor neuron-enriched cultures but also counteracted the increase of NCX reverse mode induced by SOD1 (**Fig. 4A and C**) or ApoSOD1 (**Fig. 4B and C**). Of interest, SOD1 and ApoSOD1 enhanced ER Ca^{2+} content that was measured at cytosolic level after the perfusion of the sarco(endo)plasmic reticulum ATPase inhibitor thapsigargin in the presence of EGTA (**Fig. 4D and E**). Interestingly, SOD1-induced ER Ca^{2+} accumulation as well as ApoSOD1-induced ER Ca^{2+} increase were prevented in motor neurons treated with siNCX1 (**Fig. 4D**).

Neuroprotective localization and phosphorylation of Akt induced by SOD1 and ApoSOD1 depend on NCX1 activation

To clarify the neuroprotective role of NCX1 activation, Akt localization and expression were studied in primary motor neurons exposed to SOD1 or ApoSOD1. **Figure 5A** shows a peculiar nuclear localization of active Akt (phospho-Akt, p-Akt) in a subset of MAP2-positive neurons rapidly exposed to SOD1 or ApoSOD1. Interestingly, Western blot analysis showed that SOD1- and ApoSOD1-induced p-Akt overexpression was prevented in primary motor neurons silenced for NCX1 (**Fig. 5B**). In accordance with these results, siNCX1 prevented both SOD1 and ApoSOD1-induced neuroprotection in primary motor neurons exposed to the neurotoxin L-BMAA (300µM/48h) (**Fig. 5C**). Indeed, the participation of NCX1 was further confirmed by the neuroprotective effect of the specific activator of the exchanger isoform CN-PYB2 (*26*) that prevented L-BMAA-induced cell death in motor neuron-enriched cultures (**Fig. 5C**).

Collectively, our results demonstrated the important role played by NCX1 in triggering SOD1- and ApoSOD1-dependent prosurvival pathway.

Discussion

With the aim to identify new druggable targets in ALS, the present study provides a comprehensive analysis of the upstream mechanisms underlying SOD1-induced neuroprotection in an in vitro model of the disease. Here, we tested the involvement of P_2X_7, NCX, and cADPR, three ionic proteins mainly involved in neuronal $[Ca^{2+}]i$ handling and possibly mediating the toxic effect of L-BMAA. For instance, the lack of P_2X_7 aggravates ALS symptoms by determining gliosis and motor neuron death (*27-31*). Furthermore, NCX dysfunction intervenes in ALS pathogenesis while its activation may prolong life span of $SOD1^{G93A}$ mice through the attenuation of motor neuron loss (*22, 32*). On the other hand, cADPR causes Ca^{2+} mobilization (*33*) through a direct or indirect release from ER (*34*). Moreover, in L-BMAA-treated cultures SOD1 produced neuroprotective effects in a Ca^{2+}-related way and independently from its catalytic activity (*12*). Accordingly, its free-metal form ApoSOD1 may mimic SOD1 effect in L-BMAA-treated cultures by promoting a Ca^{2+}-dependent activation of ERK1/2 and Akt and preventing ER stress-induced cell death (*12*). Among the ionic mechanisms investigated, we identified the bi-directional ion transporter NCX1 as the unique protein underlying SOD1- and ApoSOD1-induced $[Ca^{2+}]_i$ increase and, therefore, involved in their prosurvival effects. Patch-clamp experiments revealed that SOD1 as well ApoSOD1 promoted a rapid activation of NCX1 in the reverse mode of operation thus eliciting a significant increase in ER Ca^{2+} content. This possibly counteracted ER Ca^{2+} leak induced by L-BMAA thus delaying ER stress. Of particular interest is that NCX plays a crucial role against ER stress in other neurodegenerative disease including stroke and Alzheimer's disease (*17, 18, 35, 36*). This seems to be due to the ability of the exchanger to counteract Ca^{2+} leak of the most relevant Ca^{2+}-storing organelle and, therefore, to hamper the transductional cascade of ER stress. In fact, in *in vitro* model of stroke, augmented ER Ca^{2+} refilling was mediated by NCX1 working in the reverse mode (*17*). The same may occur in cortical neurons exposed to ischemic preconditioning able to induce tolerance against a subsequent harmful stimulus (*18*). This suggests that the antiporter is crucial for counterbalance the ER Ca^{2+} dysfunction induced by hypoxia in neurons.

Besides its role in mediating the upstream Ca^{2+} increase, NCX expression is regulated by most of the transductional elements activated by SOD1 and ApoSOD1 in motor neurons (*12, 37, 38*). On the other hand, by a feedback mechanism, the same transduction elements are modulated by NCX function (*12, 39*). This is consistent with the possible long-lasting participation of NCX1 in the transductional cascade underlying the neuroprotective effects of SOD1. In this context, our data showed a peculiar nuclear localization of active Akt in a subset of MAP2-positive neurons exposed to SOD1 as well as ApoSOD1. Interestingly, all Akt forms (i.e. Akt1/2/3) have been reported to reside in the nucleus or to migrate into the nucleus in response to a variety of protective stimuli in order to block apoptotic machinery or to induce the expression of those genes involved in cell survival (*40*).

Moreover, the relevance of NCX1 at motor neuron level was confirmed by the neuroprotective effect exerted by the new selective pharmacological activator of NCX1, CN-PYB2 (*26*), in L-BMAA-treated motor neurons.

Furthermore, we showed that in SBFI-loaded motor neurons, SOD1 (400 ng/mL) as well as ApoSOD1 (400 ng/mL) induced a significant increase in $[Na^+]_i$. In this respect, we reasoned that this ionic mechanism could be useful to potentiate SOD1-induced activation of NCX1 in the reverse mode of operation. Therefore, it is possible that SOD1 and ApoSOD1 interfered with the

Na+-dependent NCX1 function by the modulation of other sodium transporters expressed in motor neuron plasma membrane. In this respect, reduced Na^+/K^+ ATPase-α3 activity has been observed in animal models of ALS as well as its reduced levels in the spinal cord of both sporadic and familial ALS patients (*41*). In addition, the pharmacological inhibition of Na^+/K^+ ATPase-α3 is able to worsen disease pathology, thus confirming that an early Na+-dependent hyperexcitability is neuroprotective in ALS (*42*).

Collectively, this study shows that the initial phase of the complex mechanism shared by SOD1 and its non-metalled form ApoSOD1 in ALS/PDC model passed through the activation of NCX1 reverse mode/ER Ca^{2+} refilling and nuclear Akt activation.

Conclusions

In the present study the Na+/Ca2+ exchanger isoform 1 (NCX1) has been identified as the main upstream mechanism underlying SOD1-induced neuroprotection in an in vitro model of ALS. In this model P2X7 receptor and cADP-ribose receptor seemed to be not involved. Under basal conditions, a significant co-localization between NCX1 and endogenous SOD1 was observed at plasma membrane level in a motor neuron-enriched culture. Transductionally, SOD1 and ApoSOD1 elicited the activation of NCX1 in the reverse mode of operation favoring Ca^{2+} influx via a previous increase in $[Na^+]_i$. Then, NCX1 recharged ER of Ca^{2+} determining Akt phosphorylation and its nuclear translocation in a subset of primary motor neurons. Furthermore pharmacological activation of NCX1 protected motor neurons from the toxic effect of L-BMAA thus showing a good profile as a new candidate for pioneering ALS treatment.

List of Abbreviations

$[Ca^{2+}]_i$: intracellular calcium concentration

ER: endoplasmic reticulum

SOD1: Cu,Zn-superoxide dismutase

NCX1: Na^+/Ca^{2+} exchanger isoform 1

NCX3: Na^+/Ca^{2+} exchanger isoform 3

I_{NCX}: NCX currents

L-BMAA: hydrochloride/β-N-methylamino-l-alanine

ALS: Amyotrophic Lateral Sclerosis

MTT: 3-(4,5-dimethylthiazol-2-yl)-2,5, diphenyltetrazolium bromide

Fura-2: (1-[2-(5-carboxyoxal-2-yl)-6-aminobenzofuran-5-oxyl]-2-(2'-a mino-5'-methylphenoxy)-ethane-N,N,N',N'-tetraacetic acid)

SBFI-AM: 1,3-Benzenedicarboxylic acid, 4,4'-[1,4,10-trioxa-7,13-diazacyclopentadecane-7,13-diylbis(5-methoxy-6,12-benzofurandiyl)]bis-, tetrakis[(acetyloxy)methyl] ester

Declaration section

Ethical Approval and Consent to participate

All the procedures were performed according to the experimental protocols approved by the Ethical Committee of "Federico II" University of Naples, Italy, and according to the guidelines and regulations by Italian Ministry of Health (D.Lgs. March 4th, 2014 from Italian Ministry of Health and DIR 2010/63 from UE). The authors declare consent to participate.

Consent for publication

Not applicable.

Availability of data and materials

All raw data are available on request.

Competing interests

The authors declare no competing interests.

Funding

This work was supported by the Italian Ministry of Education, University and Research (PRIN2015–Prot. 2015KRYSJN), Progetto Speciale di Ateneo (CA.04_CDA_n_103 27.03.2019) and FRA.Linea.A.2020 (DR.2020.2449) to AS.

Authors' contributions

Conceptualization: A.S.; Methodology: T.P., V.T., V.dR., A.P., F.B. Formal Analysis: V.T., F.B.; Investigation: A.S., V.T., V.dR., T.P.; A. P. Data Curation: T.P., A.S., V.T., F.B. Writing-Original Draft Preparation: A.S.; T.P., F.B.; Writing-Review & Editing, A.S., L.A. Funding Acquisition, A.S. All authors read and approved the final manuscript.

Acknowledgements

The authors would thank Francesco Frecentese and Ferdinando Forino for participating to the synthesis of CN-PYB2.

Author information

Affiliations

1 Division of Pharmacology, Department of Neuroscience, Reproductive and Odontostomatological Sciences, School of Medicine, "Federico II" University of Naples, Via S. Pansini 5, 80131, Naples, Italy

Tiziana Petrozziello, Francesca Boscia, Valentina Tedeschi, Anna Pannaccione, Valeria de Rosa, Agnese Secondo

2 Department of Pharmacy, School of Medicine, University of Naples Federico II, Naples, Italy

Angela Corvino, Beatrice Severino

1. IRCCS SDN, Naples, Italy

Lucio Annunziato

Correspondence:

Agnese Secondo; secondo@unina.it; Tel.: +39-081-7463335

References

1. Chou SM, "Pathology-light microscopy of amyotrophic lateral sclerosis" in *Handbook of Amyotrophic Lateral Sclerosis*, R. A. Smith, Ed.(Marcel Deckker Inc, New York, NY, 1992), pp 133–181.
2. Rowland LP, Shneider NA. Amyotrophic lateral sclerosis. N Engl J Med. 2001; 344: 1688–1700 .
3. Prell T, Lautenschläger J, Grosskreutz J. Calcium-dependent protein folding in amyotrophic lateral sclerosis. Cell Calcium. 2013; 54: 132–143.
4. Lautenschlaeger J, Prell T, Grosskreutz J. Endoplasmic reticulum stress and the ER mitochondrial calcium cycle in amyotrophic lateral sclerosis. Amyotroph Lateral Scler. 2012; 13: 166–177.
5. Tadic V, Prell T, Lautenschlaeger J, Grosskreutz J. The ER mitochondria calcium cycle and ER stress response as therapeutic targets in amyotrophic lateral sclerosis. Front Cell Neurosci. 2014;8: 147-163.
6. Rosen DR, Siddique T, Patterson D, Figlewicz DA, Sapp P, Hentati A. Mutations in Cu/Zn superoxide dismutase gene are associated with familial amyotrophic lateral sclerosis. Nature**.** 1993; 362: 59–62.
7. Renton AE, Chiò A, Traynor BJ. State of play in amyotrophic lateral sclerosis genetics. Nat Neurosci. 2014; 17: 17–23.
8. Ajroud-Driss S, Siddique T. Sporadic and hereditary amyotrophic lateral sclerosis (ALS). Biochim Biophys Acta**.** 2015; 1852: 679–684.
9. Proctor E, Fee L, Tao Y, Redler RL, Fay J, Zhang Y, et al. Nonnative SOD1 trimer is toxic to motor neurons in a model of amyotrophic lateral sclerosis. Proc Natl Acad Sci**.** 2016; 113: 614–619.
10. Turner BJ, Atkin JD, Farg MA, Zang DW, Rembach A, Lopes EC, et al. Impaired extracellular secretion of mutant superoxide dismutase 1 associates with neurotoxicity in familial amyotrophic lateral sclerosis. J Neurosci**.** 2005;25: 108–117.
11. Nishitoh H, Kadowaki H, Nagai A, Maruyama T, Yokota T, Fukutomi H, et al. ALS-linked mutant SOD1 induces ER stress- and ASK1-dependent motor neuron death by targeting Derlin-1. Genes Dev**.** 2008; 22: 1451–1464.
12. Petrozziello T, Secondo A, Tedeschi V, Esposito A, Sisalli MJ, Scorziello A, et al. ApoSOD1 lacking dismutase activity neuroprotects motor neurons exposed to beta-methylamino-L-alanine through the Ca^{2+}/Akt/ERK1/2 prosurvival pathway. Cell Death Differ. 2017; 24: 511–522.
13. McGuire V, Nelson LM. "Epidemiology of ALS" in *Amyotrophic Lateral Sclerosis*, H. Mitsumoto, S. Przedborski, P. H. Gordon, Eds. (Taylor & Francis, New York, NY, USA, 2006), pp 17–41.
14. Adinolfi E, Callegari MG, Cirillo M, Pinton P, Giorgi C, Cavagna D,et al. Expression of the P2X7 receptor increases the Ca^{2+} content of the endoplasmic reticulum, activates NFATc1, and protects from apoptosis. J Biol Chem**.** 2009; 284: 10120–10128.
15. Lee HC. Cyclic ADP-ribose and NAADP: fraternal twin messengers for calcium signaling. *Sci* China Life Sci. 2011; 54**:** 699–711.
16. D'Errico S, Borbone N, Catalanotti B, Secondo A, Petrozziello T, Piccialli I, et al. Synthesis and Biological Evaluation of a New Structural Simplified Analogue of cADPR, a Calcium-Mobilizing Secondary Messenger Firstly Isolated from Sea Urchin Eggs. Mar Drugs**.** 2018; 16: 89–102.

17. Sirabella R, Secondo A, Pannaccione A, Scorziello A, Valsecchi V, Adornetto A, et al. Anoxia-induced NF-kappaB-dependent upregulation of NCX1 contributes to Ca^{2+} refilling into endoplasmic reticulum in cortical neurons. Stroke**.** 2009; 40: 922–929.
18. Sisalli MJ, Secondo A, Esposito A, Valsecchi V, Savoia C, Di Renzo GF et al. Endoplasmic reticulum refilling and mitochondrial calcium extrusion promoted in neurons by NCX1 and NCX3 in ischemic preconditioning are determinant for neuroprotection. Cell Death Differ. 2014; 21: 1142–1149.
19. Yiangou Y, Facer P, Durrenberger P, Chessell IP, Naylor A, Bountra C, et al. COX-2, CB2 and P2X7-immunoreactivities are increased in activated microglial cells/macrophages of multiple sclerosis and amyotrophic lateral sclerosis spinal cord. BMC Neurol**.** 2006; 6: 12–25.
20. D'Ambrosi N, Finocchi P, Apolloni S, Cozzolino M, Ferri A, Padovano V et al. The proinflammatory action of microglial P2 receptors is enhanced in SOD1 models for amyotrophic lateral sclerosis. J Immunol. 2009; 183: 4648–4656.
21. Gandelman M, Peluffo H, Beckman JS, Cassina P, Barbeito L. Extracellular ATP and the P2X7 receptor in astrocyte-mediated motor neuron death: implications for amyotrophic lateral sclerosis. J Neuroinflammation**.** 2010; 7: 33–41.
22. Anzilotti S, Brancaccio P, Simeone G, Valsecchi V, Vinciguerra A, Secondo A, et al. Preconditioning, induced by sub-toxic dose of the neurotoxin L-BMAA, delays ALS progression in mice and prevents Na^{+}/Ca^{2+} exchanger 3 downregulation. Cell Death Dis. 2018**;** 9: 206–222.
23. Bartlett R, Stokes L, Sluyter R. The P2X7 receptor channel: recent developments and the use of P2X7 antagonists in models of disease. Pharmacol Rev**.** 2014; 66: 638–675.
24. Rakovic S, Cui Y, Iino S, Galione A, Ashamu GA, Potter BV, et al. An antagonist of cADP-ribose inhibits arrhythmogenic oscillations of intracellular Ca^{2+} in heart cells. J Biol Chem**.** 1999; 274: 17820–17827.
25. Secondo A, Pannaccione A, Molinaro P, Ambrosino P, Lippiello P, Esposito A, et al. Molecular pharmacology of the amiloride analog 3-amino-6-chloro-5-[(4-chloro-benzyl)amino]-n-[[(2,4-dimethylbenzyl)-amino]iminomethyl]-pyrazinecarboxamide (CB-DMB) as a pan inhibitor of the Na^{+}-Ca^{2+} exchanger isoforms NCX1, NCX2, and NCX3 in stably transfected cells. J Pharmacol Exp Ther. 2009; 331: 212–221.
26. Natale S, Anzilotti S, Petrozziello T, Ciccone R, Serani A, Calabrese L, et al. Genetic Up-Regulation or Pharmacological Activation of the Na^{+}/Ca^{2+} Exchanger 1 (NCX1) Enhances Hippocampal-Dependent Contextual and Spatial Learning and Memory. Mol Neurobiol. 2020; 57: 2358–2376.
27. Valdmanis PN, Kabashi E, Dion PA, Rouleau GA. ALS predisposition modifiers: knock NOX, who's there? SOD1 mice still are. Eur J Hum Genet. 2008; 16: 140–142.
28. Apolloni S, Parisi C, Pesaresi MG, Rossi S, Carrì MT, Cozzolino M, et al. The NADPH oxidase pathway is dysregulated by the P2X7 receptor in the SOD1-G93A microglia model of amyotrophic lateral sclerosis. J Immunol**.** 2013; 190: 5187–5195.
29. Kim SU, Park YH, Min JS, Sun HN, Han YH, Hua JM, et al. Peroxiredoxin I is a ROS/p38 MAPK-dependent inducible antioxidant that regulates NF-κB-mediated iNOS induction and microglial activation. J Neuroimmunol**.** 2013; 259: 26–36.
30. Apolloni S, Amadio S, Parisi C, Matteucci A, Potenza RL, Armida M,et al. Spinal cord pathology is ameliorated by P2X7 antagonism in a SOD1-mutant mouse model of amyotrophic lateral sclerosis. Dis Model Mech**.** 2014; 7: 1101–1109.
31. Ruiz-Ruiz C, Calzaferri F, García A G. P2X7 Receptor Antagonism as a Potential Therapy in Amyotrophic Lateral Sclerosis. Front Mol Neurosci**.** 2020; 13: 93-105.

32. Mühling T, Duda J, Weishaupt JH, Ludolph AC, Liss B. Elevated mRNA-levels of distinct mitochondrial and plasma membrane Ca(2+) transporters in individual hypoglossal motor neurons of endstage SOD1 transgenic mice. Front Cell Neurosci**.** 2014; 8: 353-366.
33. Clapper DL, Walseth TF, Dargie PJ, Lee HC. Pyridine nucleotide metabolites stimulate calcium release from sea urchin egg microsomes desensitized to inositol trisphosphate. J Biol Chem**.** 1987; 262: 9561–9568.
34. Thai TL, Arendshorst WJ. Mice lacking the ADP ribosyl cyclase CD38 exhibit attenuated renal vasoconstriction to angiotensin II, endothelin-1, and norepinephrine. Am J Physiol Renal Physiol**.** 2009; 297: F169–F176.
35. Secondo A, Staiano RI, Scorziello A, Sirabella R, Boscia F, Adornetto A,et al. BHK cells transfected with NCX3 are more resistant to hypoxia followed by reoxygenation than those transfected with NCX1 and NCX2: possible relationship with mitochondrial membrane potential. Cell Calcium. 2007; 42: 521–535.
36. Pannaccione A, Secondo A, Molinaro P, D'Avanzo C, Cantile M, Esposito A,et al. A new concept: Aβ1–42 generates a hyperfunctional proteolytic NCX3 fragment that delays caspase-12 activation and neuronal death. J Neurosci**.** 2012; 32: 10609–10617.
37. Formisano L, Saggese M, Secondo A, Sirabella R, Vito P, Valsecchi V, et al. The two isoforms of the Na^+/Ca^{2+} exchanger, NCX1 and NCX3, constitute novel additional targets for the prosurvival action of Akt/protein kinase B pathway. Mol Pharmacol**.** 2008; 73: 727–737.
38. Sirabella R, Secondo A, Pannaccione A, Molinaro P, Formisano L, Guida N, et al. ERK1/2, p38, and JNK regulate the expression and the activity of the three isoforms of the Na^+/Ca^{2+} exchanger, NCX1, NCX2, and NCX3, in neuronal PC12 cells. J Neurochem**.** 2012; 122: 911–922.
39. Molinaro P, Pannaccione A, Sisalli MJ, Secondo A, Cuomo O, Sirabella R, et al. A new cell-penetrating peptide that blocks the autoinhibitory XIP domain of NCX1 and enhances antiporter activity. Mol Ther. 2015; 23: 465–476.
40. Martelli AM, Tabellini G, Bressanin D, Ognibene A, Goto K, Cocco L,et al. The emerging multiple roles of nuclear Akt. Biochim Biophys Acta**.** 2012; 1823: 2168–2178.
41. Ruegsegger C, Maharjan N, Goswami A, Filézac de L'Etang A, Weis J, et al. Aberrant association of misfolded SOD1 with Na(+)/K(+)ATPase-α3 impairs its activity and contributes to motor neuron vulnerability in ALS. Acta Neuropathol**.** 2016; 131: 427–451.
42. Saxena S, Roselli F, Singh K, Leptien K, Julien J P, Gros-Louis F, et al. Neuroprotection through excitability and mTOR required in ALS motoneurons to delay disease and extend survival. Neuron. 2013; 80: 80–96.
43. Graber DJ, Harris BT. Purification and culture of spinal motor neurons from rat embryos. Cold Spring Harb Protoc. 2013; 319–326.
44. Cashman N, Durham HD, Blusztajn JK, Oda K, Tabira T, Shaw IT, et al. Neuroblastoma x spinal cord (NSC) hybrid cell lines resemble developing motor neurons. Dev Dyn**.** 1992; 194: 209–221.
45. Grynkiewicz G, Poenie M, Tsien RY. A new generation of Ca^{2+} indicators with greatly improved fluorescence properties. J Biol Chem**.** 1985; 260: 3440–3450.
46. Urbanczyk J, Chernysh O, Condrescu M, Reeves JP. Sodium–calcium exchange does not require allosteric calcium activation at high cytosolic sodium concentrations. J Physiol**.** 2006; 575: 693–705.

47. Molinaro P, Cuomo O, Pignataro G, Boscia F, Sirabella R, Pannaccione A, et al. Targeted disruption of Na^+/Ca^{2+} exchanger 3 (NCX3) gene leads to a worsening of ischemic brain damage. J Neurosci**.** 2008; 28: 1179–1184.
48. Molinaro P, Viggiano D, Nisticò R, Sirabella R, Secondo A, Boscia F, et al. Na^+–Ca^{2+} exchanger (NCX3) knock-out mice display an impairment in hippocampal long-term potentiation and spatial learning and memory. J Neurosci**.** 2011; 31: 7312–7321.
49. Boscia F, D'Avanzo C, Pannaccione A, Secondo A, Casamassa A, Formisano L, et al. Silencing or knocking out the Na^+/Ca^{2+} exchanger-3 (NCX3) impairs oligodendrocyte differentiation. Cell Death Differ**.** 2012; 19: 562–572.
50. Secondo A, Esposito A, Petrozziello T, Boscia F, Molinaro P, Tedeschi V, et al. Na^+/Ca^{2+} exchanger 1 on nuclear envelope controls PTEN/Akt pathway via nucleoplasmic Ca^{2+} regulation during neuronal differentiation. Cell Death Discov**.** 2018; 4: 12–25.
51. Bradford MM. A rapid and sensitive method for the quantitation of microgram quantities of protein utilizing the principle of protein-dye binding. Anal Biochem**.** 1976; 72: 248–254.

Figures

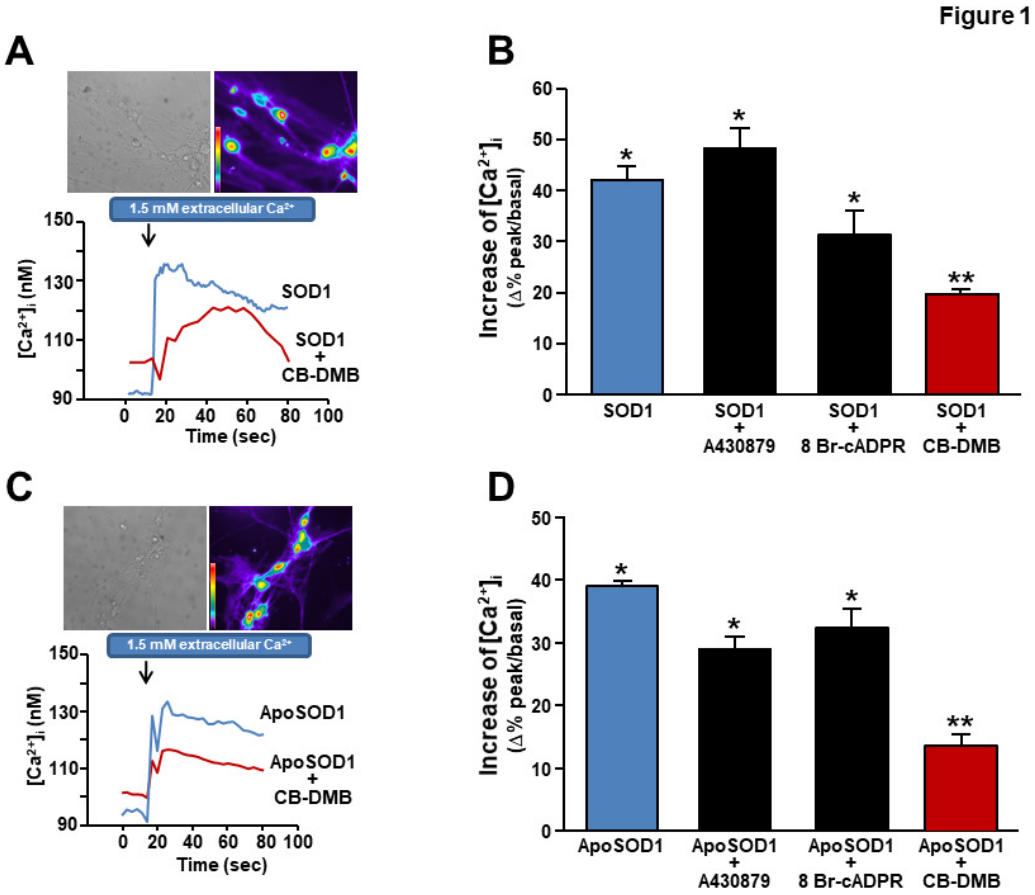

Fig. 1. Effect of the pharmacological inhibitors of P_2X_7, cADP-ribose and NCX on SOD1- and ApoSOD1-induced $[Ca^{2+}]_i$ increase in rat primary motor neurons. (**A**) Superimposed representative traces of the effect on $[Ca^{2+}]_i$ of SOD1 alone (400 ng/ml) or in combination with CB-DMB (1 μM) in Fura-2-loaded primary motor neurons. (**B**) Quantification of the effect of SOD1 (400 ng/ml) alone (n=30 cells) and in the presence of CB-DMB (1 μM) (n=25 cells), the specific antagonist of P_2X_7 receptor, A430879 (1 μM) (n=35 cells) or the cell permeant antagonist of cADP-ribose, 8-bromo-cADPR (10 μM) (n=28 cells). Primary motor neurons were pre-incubated with CB-DMB, A430879 or CB-DMB for 10 minutes before $[Ca^{2+}]_i$ recordings. All the experiments were repeated at least three times; *$p < 0.05$ vs internal control (basal values of $[Ca^{2+}]_i$), **$p < 0.05$ vs internal control and SOD1 alone. (**C**) Superimposed representative traces of the effect on $[Ca^{2+}]_i$ of ApoSOD1 alone (400 ng/ml) or in combination with CB-DMB (1 μM) in Fura-2-loaded primary motor neurons. (**D**) Quantification of the effect of ApoSOD1 (400 ng/ml) alone (n=29 cells) and in the presence of CB-DMB (1 μM) (n=30 cells), the specific antagonist of P_2X_7 receptor, A430879 (1 μM) (n=35 cells) or the cell permeant antagonist of cADP-ribose, 8-bromo-cADPR (10 μM) (n=30 cells). Primary motor neurons were pre-incubated with CB-DMB, A430879 or CB-DMB for 10 minutes before $[Ca^{2+}]_i$ recordings. All the experiments were repeated at least three times on different cultures; *$p < 0.001$ vs internal control (basal values of $[Ca^{2+}]_i$), **$p < 0.05$ vs internal control and ApoSOD1 alone.

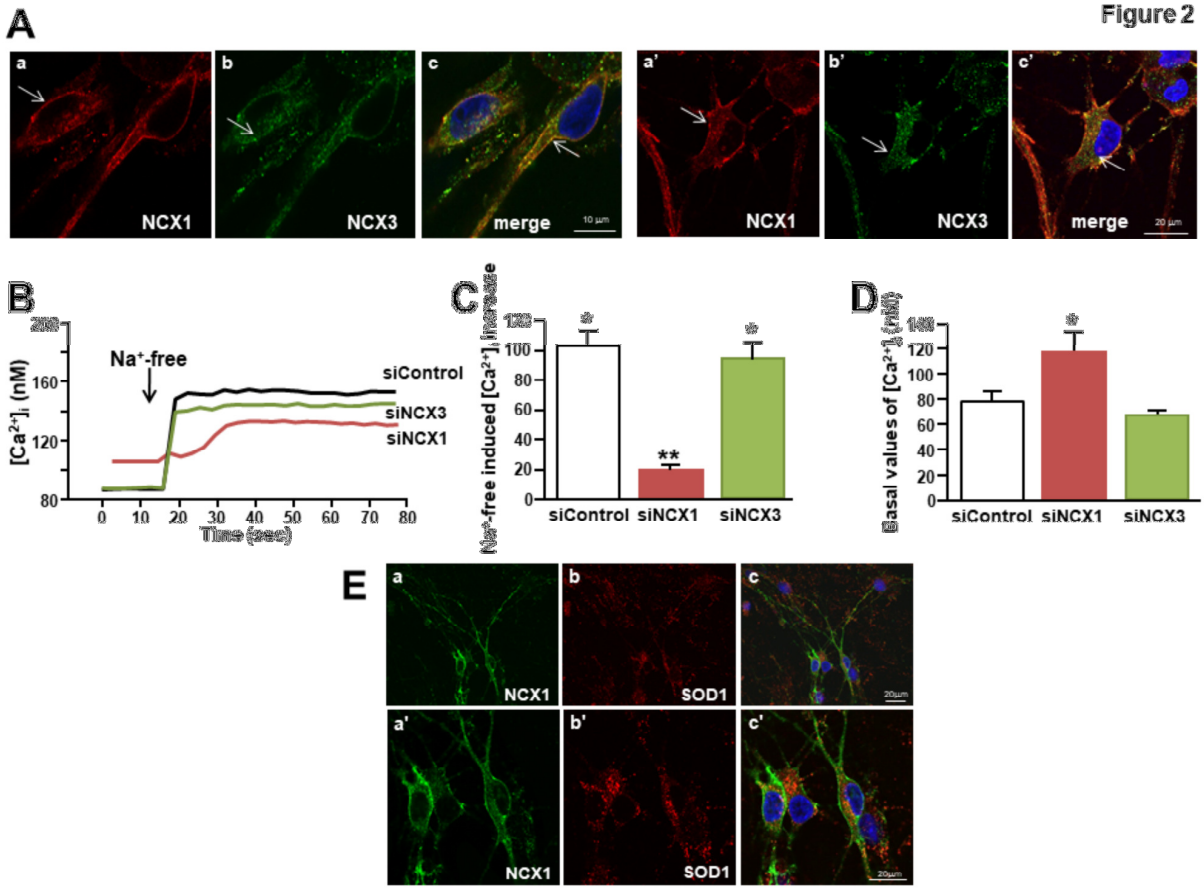

Fig. 2. NCX1 and NCX3 expression and function in rat primary motor neurons. (**A**) Immunolocalization of NCX1 and NCX3 isoforms in two different motor neurons within the same culture. Scale bars: 10 µm (a, b, c), 20 µm (a', b', c'). (**B**) Superimposed representative traces of the effect of Na^+-free on $[Ca^{2+}]_i$ in motor neurons singly transfected with siControl, siNCX1 or siNCX3 (both at 10 nmol/L for 48 h). For details, please refer to Material and Methods. (**C**) Quantification of A expressed as Δ% of increase. All the experiments were repeated at least three times; *$p < 0.001$ vs internal control (basal values of $[Ca^{2+}]_i$), **$p < 0.05$ vs siControl and siNCX3. (**D**) Quantification of basal values of $[Ca^{2+}]_i$ of the treatments of A. *$p < 0.05$ vs all. (**E**) Immunolocalization of NCX1 and SOD1 in a field of motor neuron-enriched culture at two different magnifications.

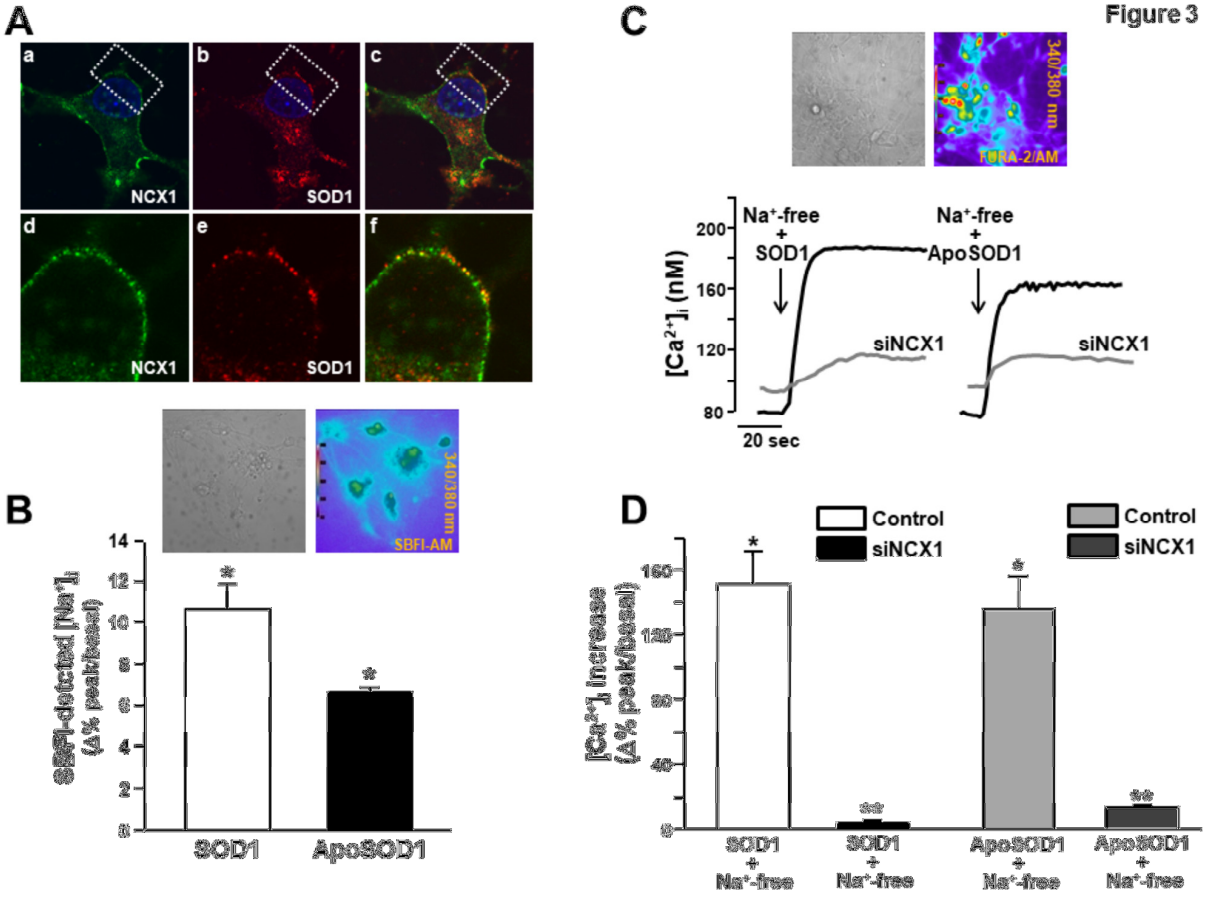

Fig. 3. Effect of SOD1 and ApoSOD1 on NCX1-mediated $[Ca^{2+}]_i$ influx and $[Na^+]_i$ in rat primary motor neurons. (**A**) Co-localization between plasmalemmal NCX1 and SOD1 in a representative rat primary motor neuron at two different magnifications. (**B**) Quantification of SOD1 and ApoSOD1-induced $[Na^+]_i$ increase in SBFI-loaded motor neurons (see representative images on the top). Data are quantified as Δ% of increase in 35 cells for each group. All experiments were repeated at least three times; *$p < 0.05$ vs internal control (basal values of $[Na^+]_i$). (**C**) Superimposed representative traces of the effect on $[Ca^{2+}]_i$ of SOD1 (400 ng/ml) in Na^+-free solution and ApoSOD1 (400 ng/ml) in Na^+-free solution both perfused on siControl neurons or siRNA-treated neurons against NCX1 (10 nmol/L for 48 h) loaded with Fura-2 (see representative images on the top). (**D**) Quantification of the effect of C reported as Δ% of increase in 40 cells for each group. All the experiments were repeated at least three times; *$p < 0.001$ vs SOD1 or ApoSOD1 alone (in the presence of external Na^+); **$p < 0.05$ vs "SOD1+Na^+-free" or "ApoSOD1+Na^+-free".

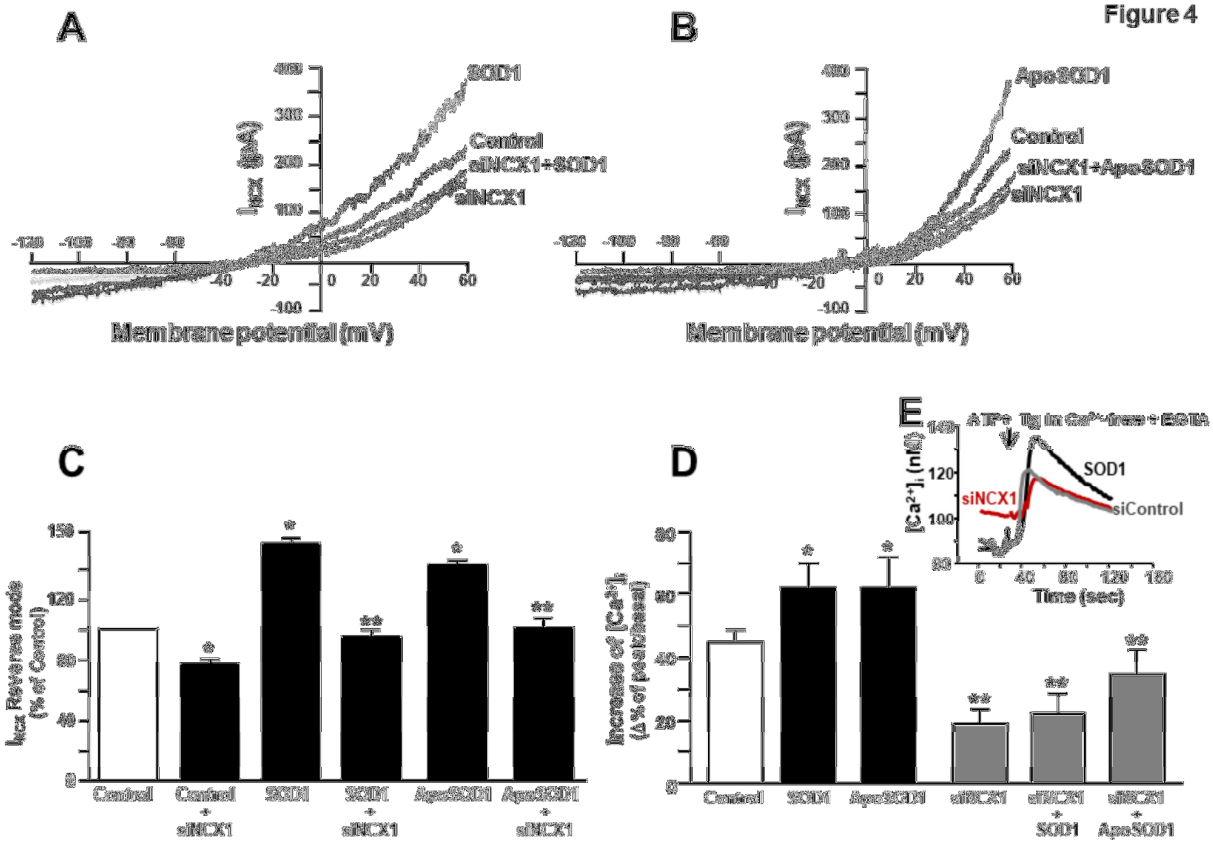

Fig. 4. Effect of SOD1 and ApoSOD1 on NCX1-mediated currents (I_{NCX}) and ER Ca^{2+} content in rat primary motor neurons. (**A**) Superimposed traces of I_{NCX} recorded by patch-clamp in rat primary motor neurons perfused with SOD1 and previously transfected with siControl (control) or siRNA against NCX1 (siNCX1; 10 nmol/L for 48 h). (**B**) Superimposed traces of I_{NCX} recorded by patch-clamp in rat primary motor neurons perfused with ApoSOD1 and previously transfected with siControl (control) or siRNA against NCX1 (siNCX1). (**C**) Quantification of A (n = 20 cells for each group) and B (n = 15 cells for each group). All the experiments were repeated at least three times; *$p < 0.05$ vs siControl and untransfected cells; ** $p < 0.05$ vs SOD1 or ApoSOD1 alone. (**D**) Effect of SOD1 and ApoSOD1 on ER Ca^{2+} content in the absence or presence of siNCX1 (10 nmol/L for 48 h). ER Ca^{2+} content has been measured by ATP (100 µM) and thapsigargin (1 µM) in a Ca^{2+}-free solution containing EGTA in Fura 2-loaded motor neurons. Quantification has been reported as Δ% of increase in n=30 cells for each group recorded in 3 independent experiments. *$p<0.05$ vs control; **$P<0.05$ vs control or vs SOD1 and ApoSOD1. (**E**) Superimposed representative traces of control neurons, motor neurons exposed to SOD1 or siNCX1-transfected neurons exposed to ATP and thapsigargin in a Ca^{2+}-free solution containing EGTA as reported in panel D.

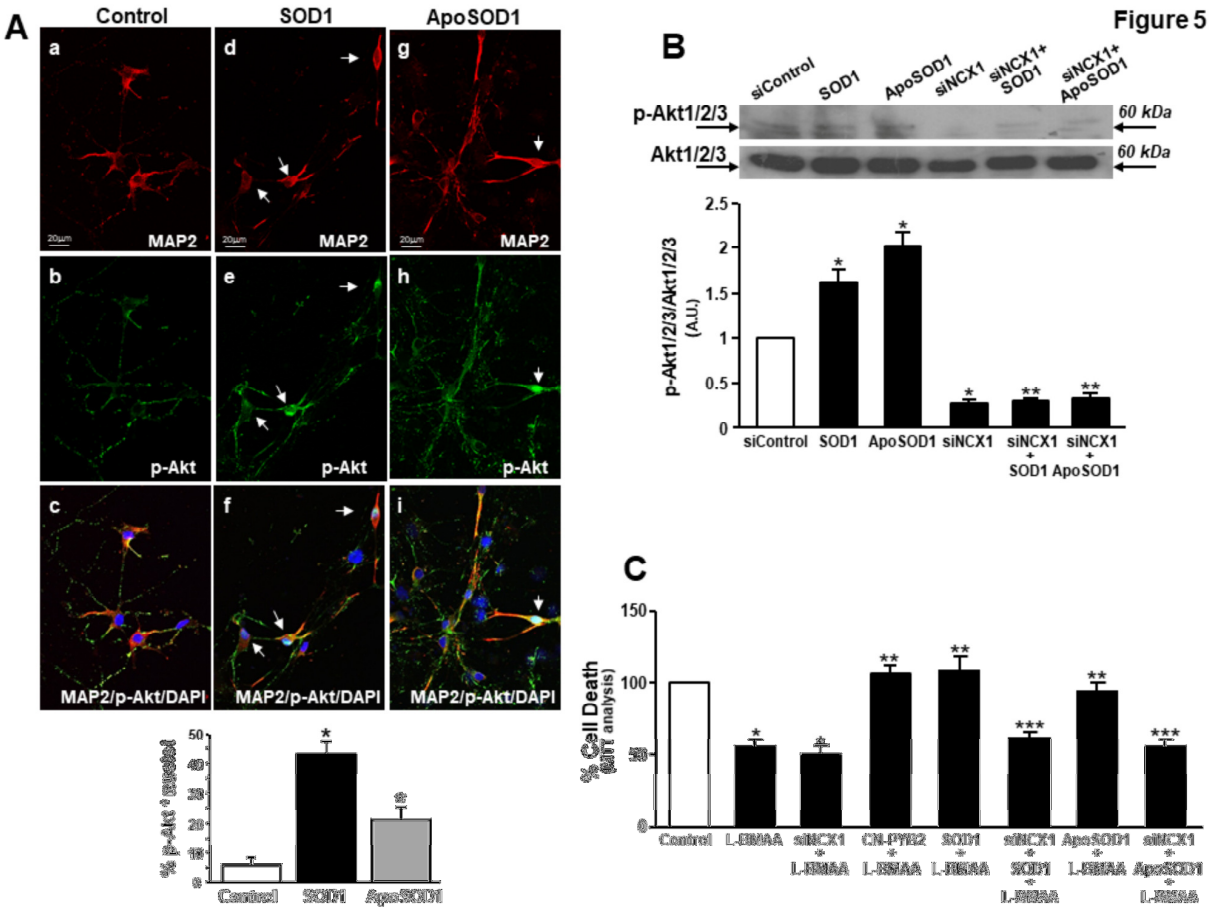

Fig. 5. Effect of SOD1 and ApoSOD1 on phospho-Akt expression and localization in rat primary motor neurons. (**A**) Immunolocalization of phospho-Akt (p-Akt) in MAP2-positive cells within a motor-neuron enriched culture under control conditions (a-c), exposed to SOD1 (400 mg/ml/10 minutes) (d-f) or ApoSOD1 (400 mg/ml/10 minutes) (g-i). Motor-neuron enriched culture were harvested before the treatment with SOD1 or ApoSOD1. White arrows indicate MAP2-neurons showing a nuclear localization of p-Akt. Bar graph at the bottom represents the % of p-Akt-positive nuclei in each of the three groups. *p<0.05 vs control. (**B**) Representative Western blotting and quantification of the effect of SOD1, and ApoSOD1 (400 ng/ml/10 min) on p-Akt and Akt1/2/3 expression in the absence or presence of siNCX1 (10 nmol/L for 48 h). Data are expressed as mean±SE of three different experimental sessions. *p<0.05 vs siControl; **p<0.05 vs siControl or vs SOD1 and ApoSOD1. (**C**) Bar graph depicting the effect of L-BMAA (300 μM/48 h) on cell death, measured by MTT, of rat primary motor neurons pretreated with SOD1, or ApoSOD1 (400 ng/ml/10 min) in the presence or absence of siNCX1 or after exposure to the NCX1 activator CN-PYB2 (10nM). Data are expressed as mean±S.E. of three different experimental sessions. *p<0.05 vs control; **p<0.05 vs L-BMAA alone; ***p<0.05 vs L-BMAA +SOD1 or L-BMAA +ApoSOD1.